Application of Acid Activated Ouw's Natural Clay (ONC) on Adsorption of Methylene Blue Dye

Catherina Manukpadang Bijang [1], Yusthinus Thobias Male [1], Shielda Natalia Joris [1,*], Crismenda Kartini Wattimena [2]

[1] Department of Chemistry, Faculty of Mathematics and Natural Sciences, Pattimura University, Ambon, Indonesia
[2] Inorganic Chemistry Laboratory, Faculty of Mathematics and Natural Sciences, Pattimura University, Ambon, Indonesia

* Corresponding authors: shieldajoris@gmail.com

Article Info

Abstract

The application of natural clay as an adsorbent has been widely used. This is supported by the porous surface texture of the clay. However, some treatments are needed to remove impurities in natural clay before using it as an adsorbent. The common effort is to activate it with acid. This research studied the effect of hydrochloric acid concentration on the adsorption capacity of methylene blue dye. The concentrations of hydrochloric acid used were 2, 3, and 4 M. Characterization was carried out with IR, XRD, and SEM-EDX spectroscopy to see the differences in ONC characters before and after adding hydrochloric acid. The characterization results showed that ONC contained montmorillonite and quartz, and an increase in base distance was directly proportional to the increase in the concentration of hydrochloric acid used. High concentrations of hydrochloric acid caused excessive dealumination and deionization. The dealumination process was supported by IR data where there was a shift in wavenumber in the Al-O stretching vibration region from 796 cm^{-1} to 794 cm^{-1}; the sharper the vibration in the Si-O region (488-468 cm^{-1}); there was also an increase in the Si/Al ratio of pure ONC from 1.7497 to 2.2970 for 3 M ONC-HCl. The concentration of hydrochloric acid did not significantly affect the capacity of ONC as an adsorbent for methylene blue. The adsorption capacity of pure ONC obtained was 4.97215 mg/g, while for ONC-HCl 3 M was 4.97746 mg/g.

1. Introduction

Natural clay in Indonesia, especially in the village of Ouw, Saparua Island, Maluku, is only used as a raw material for ceramic crafts and brick making. Based on previous research, the components contained in Ouw natural clay (ONC) are montmorillonite, quartz, kaolinite, and illite, and the most dominant is montmorillonite.

Montmorillonite can be used as an adsorbent based on its properties: wide specific surface area, chemically and mechanically stable, varied surface structures, high ion exchange capacity, and Bronsted and Lewis acids [1]. One way to improve clay's physical and chemical properties is by acid activation treatment. Activation is a process intended to enlarge the size of the pore by oxidizing the surface molecules. This results in physical and chemical changes to the adsorbent, enhancing its surface acidity and creating active sites [2]. This has been studied by Catherina et al. [3], who showed that clay activation with acid increased the surface area and distance between layers. The acid attack on clay minerals has additional effects on the mineralogical composition of the raw material and related properties; that is, organic matter is leached out, and feldspar can be partly attacked (or dissolved). This process causes an increase in surface area and surface acidity, introduces permanent mesoporosity, and removes metal ions from the crystal interlayer, which partially delaminates the clay [4].

Clay can be used as an adsorbent to adsorb dyes. One of the synthetic dyes widely used is methylene blue because it is easily soluble in water and has an economical price. This compound is relatively stable. However, its stability poses challenges for natural degradation, potentially posing risks in high concentrations [5].

Several reports on the adsorption ability of dyes by clay have been demonstrated, such as the adsorption of methylene blue on sulfuric acid-activated clay, utilization of sulfuric acid-activated ONC as an adsorbent for methylene blue, and adsorption of rhodamine B on hydrochloric acid-activated ONC [6, 7, 8, 9]. This study focuses on examining the effect of different concentrations of hydrochloric acid, used in activating Ouw natural clay, on its ability to adsorb methylene blue dye.

2. Experimental

The research process includes ONC sample preparation, activation with hydrochloric acid using varying concentrations of 2, 3, and 4 M, characterization of acid-activated ONC, making a standard solution of methylene blue, and measuring the absorbance of methylene blue using a UV-Vis spectrophotometer.

2.1. Equipment/Tools/Materials

The tools used in this research were a set of glassware (Pyrex), analytical balance (Ohaus), electric heater (Cimarec 2), magnetic stirrer, mortar and pestle, 100 mesh sieve, oven (Memmert), desiccator, shaker (GFL 3005), Vacuum pump (Vacuubrand GMBH + CO KG), UV-Vis spectrophotometer (Thermo Scientific GENESYS 10S), Infrared spectrophotometer (Prestige-21 Shimadzu), SEM-EDX (ZEISS EVO® MA 10), XRD (Bruker type D2 Phaser. The materials used in this research were Natural Clay Ouw (ONC), HCl (analytical grade, Merck), Methylene blue dye (analytical grade, Merck), $AgNO_3$, distilled water, and filter paper.

2.2. Sample Preparation

ONC samples were soaked and washed with distilled water several times, then filtered using a vacuum pump to obtain clay free of impurities such as sand, gravel, and plant roots. Subsequently, the clay was dried for 4 hours in an oven at 80°C. The dried clay was then crushed, sieved with a 100-mesh sieve, and stored in a desiccator.

2.3. Activation with Hydrochloric Acid

Three 250 mL beakers were each filled with 10 g of the prepared ONC sample, after which 100 mL of HCl solution with concentrations of 2, 3, and 4 M was added to each while stirring with a magnetic stirrer. The activation process was conducted for 24 hours, followed by filtration. The residue was washed with distilled water until the filtrate ceased to produce an AgCl precipitate when tested with an $AgNO_3$ solution. Subsequently, the clay was dried in an oven at 80°C. The dried ONC samples were then crushed and sieved using a 100-mesh sieve. Lastly, the sample was stored in a desiccator.

2.4. ONC Characterization

ONC samples were characterized using IR, XRD, and SEM-EDX. Characterization with an IR spectrophotometer was needed to determine the functional clusters and to study the profile and changes in the absorption area. XRD analysis was conducted to identify the crystal structure, while SEM-EDX characterization was utilized to examine the surface morphology and elemental composition of the samples.

2.5. Preparation of Methylene Blue (MB) Standard Solution

A 1000 ppm methylene blue stock solution was prepared by weighing 1 g of MB and adding it to a 1000 mL volumetric flask, which was then filled with distilled water up to the mark. From this stock solution, MB standard solutions of 0.2, 0.4, 0.6, 0.8, and 1.0 ppm were prepared by measuring out 0.2, 0.4, 0.6, 0.8, and 1.0 mL, respectively, and diluting each in a 10 mL volumetric flask with distilled water to the mark. The absorbance of these standard solutions was measured at a wavelength of 665 nm using a UV-Vis spectrophotometer [8]. The obtained results were used to make the standard curve.

2.6. Determination of the Effect of HCl Concentration on MB Adsorption

Initially, 0.5 g of ONC sample before and after activation was placed in each 100 mL Erlenmeyer flask. Subsequently, 50 mL of a 50 ppm MB solution was added to each flask. The mixture was then stirred using a shaker at 250 rpm for 24 hours under a pH of 7. Afterward, the mixture was filtered, and the filtrate was collected for analysis. The absorbance of the filtrate was measured using a UV-Vis spectrophotometer at a wavelength of 665 nm. Based on the UV-Vis results, the final concentration in the filtrate (C_e) was calculated, and then the percentage and adsorption capacity was determined using Equations (1) and (2).

$$Q = \frac{C_0 - C_e}{C_0} \times 100\% \qquad (1)$$

$$q = (C_0 - C_e) \times \frac{MB\ volume}{ONC\ mass} \qquad (2)$$

Where, Q is the adsorption percentage, q is the adsorption in the solid, C_0 is the initial concentration of the solution, C_e is the equilibrium concentration in the liquid phase.

3. Results and Discussion

3.1. IR Spectroscopy Characterization

The IR spectroscopic characterization aims to determine the functional clusters in pure ONC, 2, 3, and 4 M ONC-HCl samples. The IR spectra of ONC samples (Figure 1) show some typical absorption bands, which appear at 3620, 1636, 1035, 794, 530, and 468 cm^{-1}. This indicates that montmorillonite is one of the minerals composing the clay, with the structure shown in Figure 2 [7].

Based on Table 1, the appearance of absorptions in the 3697 cm^{-1} and 3622-3620 cm^{-1} indicate the presence of stretching vibrations of the OH groups. The two wavenumbers indicate a stretching OH functional cluster in the octahedral layer (aluminol) and OH stretching vibrations silanol. This is also confirmed by the emergence of a peak at 3669, 3653, and 3620 cm^{-1}, which are O-H silanol stretching vibrations or those found between the tetrahedral and octahedral layers, respectively [10]. The interpretation of the ONC sample spectrum can be seen further in Table 1.

Table 1. Spectra interpretation of ONC samples

| Wavenumber (cm⁻¹)					Functional cluster absorption
Pure ONC	2 M ONC-HCl	3 M ONC-HCl	4 M ONC-HCl	Standard comparison	
3697	3697	3697	3697	3669	O–H stretching vibration [11]
3620	3622	3622	3622	3630	O–H stretching vibration [11]
3442	3412	3414	3417	3400	O–H stretching vibration from the water molecule [12]
1641	1641	1641	1641	1633	H_2O bending vibration from the water molecule [8]
1031	1033	1033	1031	1048	Si–O and Al–O Asymmetric stretching vibration [13, 14]
910	908	908	910	91	O–H bending vibration from Al-OH-Al
796	794	794	794	820-650	Si–O and Al–O Asymmetric stretching vibration [13, 14]
536	536	536	536	520	Al–O stretching vibration [10]
488	488	486	468	470	Si–O stretching vibration [10]
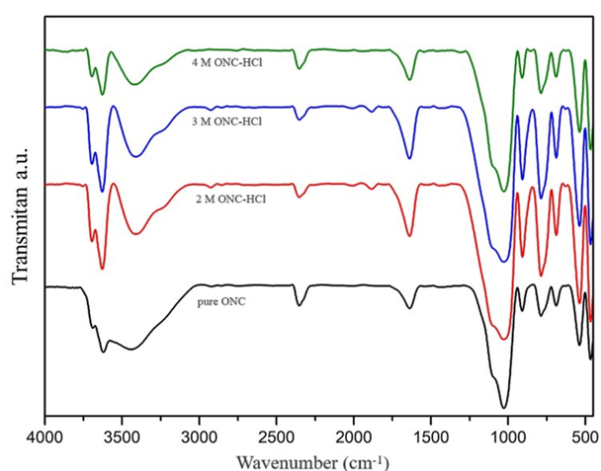
Figure 1. IR spectra of samples

The wavenumber in the 3442-3412 cm⁻¹ region indicates the OH group's stretching vibration, which the adsorbed water molecule hydrates. This is supported by an absorption band at wavenumber 1641 cm⁻¹, indicating H–O–H's bending vibrations from water adsorbed in ONC. This report aligns with that observed by Grim [12], which stated that H_2O bound to clay provides absorption in the 3400 cm⁻¹ and 1640 cm⁻¹ regions. The absorption area of 3442 cm⁻¹, namely the O–H stretching vibrations of water molecules for pure ONC samples, experienced successive shifts to 3412, 3414, and 3417 cm⁻¹ for 2, 3, and 4 M ONC-HCl samples, respectively. This was caused by releasing physically bound water molecules in the clay, making the sample pores cleaner and more open.

The presence of Si–O and Al–O groups in the ONC samples was identified by the appearance of a sharp absorption band with high intensity at 1033-1031 cm⁻¹ region. The high intensity at this peak indicates the high montmorillonite content in the clay [13, 14]. This aligns with previous studies in which the absorption bands at 1250-950 cm⁻¹ indicate an asymmetrical Si–O and Al–O stretching vibration [15, 16, 17, 18]. The Si–O and Al–O symmetrical stretching vibrations were also observed at 796-794 cm⁻¹ [13, 14]. The data follows the report states that the absorption in the area 820-650 cm⁻¹ is a symmetrical M–O stretching vibration, where M is Si and Al. This is also supported by absorption in the 500-420 cm⁻¹ region, indicating bending vibrations from Si–O and Al–O. The bending vibrations of Al–O and Si–O in ONC samples are shown at 536 cm⁻¹ and 488-468 cm⁻¹. This follows the previous report: the Al–O bending vibration occurs at the absorption area of 520 cm⁻¹, and the Si–O bending vibration at 470 cm⁻¹ [10]. The bending vibration of the hydroxyl group from Al–OH–Al also appears in the absorption band of 910 cm⁻¹.

The IR spectra of pure ONC samples and those after the addition of HCl reveal minimal discrepancies in the absorption peak wave numbers, characterized by slight shifts and subtle differences in spectral sharpness. According to Önal and Sarıkaya [19], the addition of acid to natural bentonite does not alter its fundamental structure but merely eliminates impurities.

Acid treatment causes changes in the crystalline structure of clay minerals. This can be seen in the changes in the diffractogram of acid-activated clay compared to the original clay. There is an increase in basal spacing from 4.44° to 4.47° accompanied by a reduction in intensity from 43.06 to 29.09%. The decrease in intensity indicates the reduction of octahedral and tetrahedral sides in the clay. Acid treatment gave rise to a new peak at 22.91°. This peak indicates the formation of an expanded phase and interlamellar expansion. Additionally, the effect of acid treatment is evident in the IR spectra, particularly through the notable shift in the Si–O bending group [20].

Table 2. X-ray diffraction result

| Sample	Analysis results		Information	Intensity
	2θ (°)	d (Å)		
Pure ONC	26.813	3.32232	Montmorilonite d_{103}	13756
	6.284	14.05293	Montmorilonite d_{001}	240
	20.079	4.41862	Quartz	297
2 M ONC-HCl	26.750	3.32999	Montmorillonite d_{103}	17276
	6.319	13.97626	Montmorillonite d_{001}	106
	20.018	4.43206	Quartz	201
3 M ONC-HCl	26.687	3.33769	Montmorillonite d_{103}	20015
	19.957	4.44549	Quartz	244
4 M ONC-HCl	26.650	3.34229	Montmorillonite d_{103}	17692
	5.588	15.80356	Montmorillonite d_{001}	94.1
	19.831	4.47334	Quartz	305
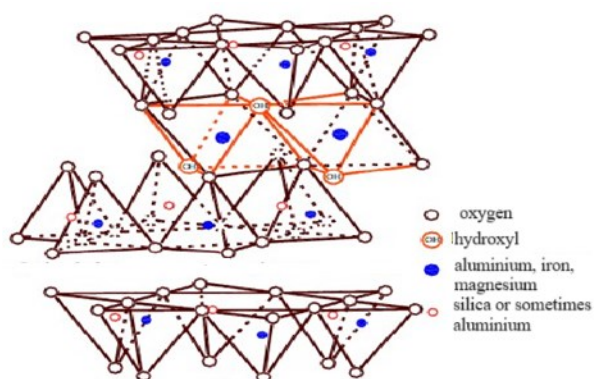
Figure 2. Montmorillonite structure
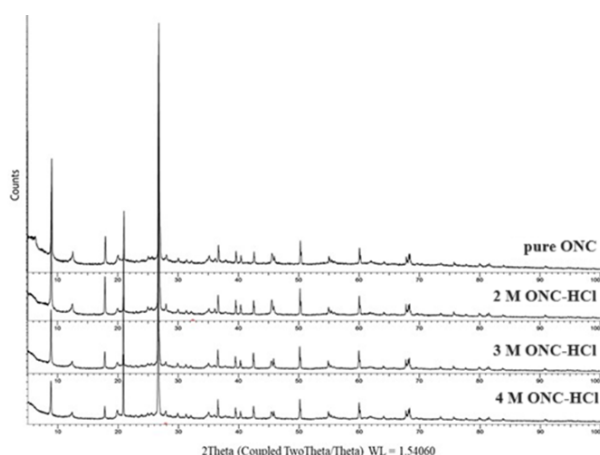
Figure 3. ONC samples diffractogram

Treatment with acid also causes dealumination, characterized by releasing Al^{3+} ions from the octahedral layer. Spectroscopically, dealumination can be observed within the wavenumber range of 1300-300 cm^{-1}, including a shift in spectral peaks associated with Al−O vibrations [18]. Based on the data presented in Table 2, dealumination effects in the Al-O vibrations are evident across three absorption regions. Initially, the absorption areas for pure ONC samples are observed at 536, 796, and 1031 cm^{-1}. Following the addition of HCl, no shift was observed in the 536 cm^{-1} region, although there was a slight difference in spectral sharpness. However, for the absorption area at 796 cm^{-1}, corresponding to the symmetric stretching vibration of Al-O, a shift to 794 cm^{-1} was observed in 2, 3, and 4 M ONC-HCl samples. Additionally, the absorption area at 1031 cm^{-1} shifted to 1033 cm^{-1} for the 2 and 3 M ONC-HCl samples, with no shift observed in the 4 M ONC-HCl sample.

The observation for the dealumination of all samples after adding HCl is indicated by the narrowing of the spectral region at 3622 cm^{-1}, corresponding to the area of O-H stretching vibrations. This is probably due to the damage to the O-H structure originating from the octahedral Al-OH due to the treatment of the clay with HCl. Treatment of clay with acid can increase the number of silanol groups (-Si-OH) and lead to cyclosan clusters (Si-O-Si) formation. These clusters were previously obscured by organic components, other metal oxides, or the replacement of Al by Si resulting from acid-induced dealumination [6]. The release of Al from Si-O-Al leads to the rearrangement of Si-O-Si bonds outside the framework. This process increases the silicon composition within the framework. This effect is noticeable in the 4 M ONC-HCl sample within the wavenumbers of 488-468 cm^{-1}, particularly in the Si-O bending vibration region, which exhibits sharper characteristics compared to the pure ONC sample.

3.2. Characterization by X-ray Diffraction

Based on the diffractogram of pure ONC samples (Figure 3), the characteristic absorption peak with the corresponding base angle and distance occurs at its highest intensity at 2θ = 26.813° (d = 3.32232 Å), consistent with JCPDS standard No. 13-0135, denoted as d = 3.30 Å, corresponding to the montmorillonite d_{103} lattice plane. The presence of montmorillonite is further supported by additional peak data. A peak at 2θ = 6.284° (d = 14.05293 Å), corresponding to JCPDS No. 13-0135, indicates montmorillonite d_{001} = 15.00 Å. Additionally,

a peak at $2\theta = 20.079°$ (d = 4.41862 Å) aligns with JCPDS No. 05-0490, corresponds to $d_{100} = 4.25$ Å, indicating the presence of quartz mineral. Therefore, the XRD characterization of pure ONC, covering an angle range of 2θ from 0 to 100°, confirms the predominant presence of montmorillonite, supported by additional minerals such as quartz.

The diffraction patterns of 2, 3, and 4 M ONC-HCl samples depicted in Figure 3 exhibit typical adsorption peaks with angles and base distances comparable to those of the pure ONC samples, as detailed in Table 2. Consequently, the constituent minerals remain unchanged: montmorillonite and quartz. A leftward shift of 2θ in montmorillonite indicates an expansion in the interlayer spacing. This expansion is attributed to dealumination induced by adding HCl, wherein Al is released from the octahedral layer, and H^+ clusters are replaced by HCl. The presence of the H^+ group facilitates the removal of metals and other impurities, resulting in a reduction in the crystallinity of ONC following the addition of HCl.

The release of Al by this acid also contributes to the increased intensity of quartz due to increased Si-O-Si bonds. While minerals composing alumina clusters may incur damage, silica sheets, characteristic of minerals like quartz, generally remain unaffected by acids due to their composition of SiO_2. This can be seen in Table 2 for the 4 M ONC-HCl sample, where there was a relatively high increase in quartz intensity and a greater chance of experiencing dealumination than the other samples. This is also supported by IR absorption data showing the dealumination process in the 4 M ONC-HCl sample, where the wavenumber region of 488-468 cm^{-1} (Si-O bending vibration) becomes sharper than the pure ONC sample. In the 3 M ONC-HCl sample, there was no d_{001} montmorillonite. This was also explained by Önal and Sarıkaya [19], where at specific acid concentrations, the characteristics of montmorillonite in the d_{001} field decreased. Nonetheless, montmorillonite in the sample remains observable in the region $2\theta = 26.687°$ (d = 3.33769 Å). The intensity of montmorillonite in this area is also much higher than in other samples.

3.3. Characterization using SEM-EDX

The SEM-EDX characterization is expected to display changes in the sample's surface morphology. Its function is to visualize and determine the surface composition of a material using the principle of electron shooting. Figure 4 shows SEM images with a magnification of 1000 times of pure ONC and 2, 3, and 4 M ONC-HCl samples.

After adding HCl, it is anticipated that the pores of the ONC sample will become more open. Figures 4(b), 4(c), and 4(d) illustrate that the pores in the sample (depicted in black) indeed become more significant. In Figure 4(a), the surface of the ONC before adding HCl reveals a scarcity of pores, represented by black holes on the sample's surface. In Figure 4(b), only a few pores are discernible. Figure 4(c) demonstrates that the surface has

become more open, smoother, and cleaner. After adding HCl, the larger pores on the ONC surface allow this material to perform better adsorption than pure ONC. In Figure 4(d), numbers of pore spaces are formed. However, as indicated by the IR and XRD data, this sample may have undergone excessive dealumination compared to others, potentially leading to a vulnerability in its crystal lattice. Further clarification on this matter is provided through EDX data analysis.

The EDX characterization is used to determine the elements present in the sample's surface morphology. Table 3 shows the main components of the clay characterized by EDX. The increase in the % Si/Al ratio from pure ONC to 3 M ONC-HCl was due to the dissolving of some aluminium on the surface and in the montmorillonite framework through the dealumination process. Dealumination causes a structural overhaul wherein aluminum sites are filled with silicon, leading to a general increase in silicon content. The Al−O bond energy value was 116 kcal/mol, and the Si−O bond energy was 184 kcal/mol, which means that the Al−O bond is weaker than the Si−O bond, so the Al−O bond easier to break after reacting with acid. The use of HCl with a greater concentration allows the dissolution of other cations, such as Mg^{2+}, Fe^{3+} which are in dioctahedral sheets, thus blocking the dissolution process of Si^{4+} and Al^{3+} in tetrahedral and octahedral positions [21].

Another factor that causes an increase in the value of the Si/Al ratio is the more electropositive nature of Al compared to Si (the electronegativity of Al is 1.5 while the electronegativity of Si is 1.8). The amount of electronegativity indicates the ability of an atom to compete for electrons with other bonded atoms. The greater the electronegativity, the stronger the bond formed. The presence of H^+ ions from the acid can influence the free electrons on the oxygen atoms, leading to the formation of coordinate bonds. Consequently, Al-O bonds may experience a reduction in electron density, rendering them more polar and comparatively weaker. As a result, the bonds holding aluminum may become susceptible to breaking.

Based on Table 4, the 2 M ONC-HCl sample experienced the highest dealumination, while the % Si/Al ratio in the 4 M ONC-HCl sample decreased. Thus, it can be concluded that the significant base distance in the XRD results was not only due to dealumination but also possibly due to the deionization of other elements in the clay.
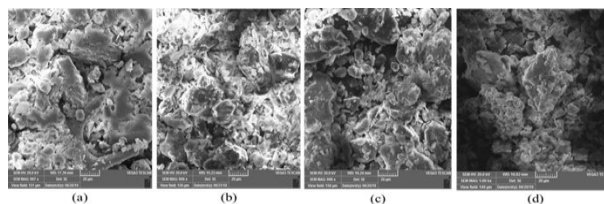

Figure 4. SEM images of (a) Pure ONC, (b) 2 M ONC-HCl, (c) 3 M ONC- HCl, and (d) 4 M ONC-HCl

Table 3. EDX data of the composition of the main constituents of the ONC sample

Sample	%Si	%Al	%Si/Al ratio	%O
Pure ONC	19.65	11.23	1.7497	61.32
2 M ONC-HCl	22.08	9.57	2.3072	61.21
3 M ONC-HCl	19.18	8.35	2.2970	60.30
4 M ONC-HCl	19.27	10.73	1.7959	64.60

Table 4. Calculation results of ONC adsorption capacity

Sample	Average absorbance	C_e (ppm)	$C_o - C_e$ (ppm)	Q (%)	q (mg/g)
Pure ONC	0.0380	0.2785	49.7215	99.44	4.97215
2 M ONC-HCl	0.0360	0.2679	49.7321	99.46	4.97321
3 M ONC-HCl	0.0280	0.2254	49.7746	99.55	4.97746
4 M ONC-HCl	0.0313	0.2429	49.7571	99.51	4.97571

Note: Q is the adsorption percentage, q is the adsorption capacity, C_o is the initial concentration of the solution, C_e is the final concentration of the solution, and $(C_o - C_e)$ is the concentration of the adsorbed solution.

3.4. Determine the Effect of HCl Concentration on Adsorption of Methylene Blue

Methylene blue (MB) adsorption was done by adding 50 mL of MB 50 ppm solution to 0.5 g ONC and stirring for 24 hours. Table 4 shows the results of calculating the adsorption capacity of ONC. The adsorption in this study was physical adsorption, which occurred on the pore surface of the ONC sample. Based on the XRD data, the sample bottom distance value increases in direct proportion to the increase in HCl concentration, which means that the pores produced after adding HCl become cleaner, increasing the surface area.

Table 4 shows ONC's adsorption capacity, and percentage after HCl activation did not show significant changes. Using a small amount of adsorbent causes MB adsorbate with a concentration of 50 ppm and a volume of 50 mL to be maximally absorbed by 0.5 g of ONC. Therefore, the adsorbent mass must be increased to obtain a significant change. Although the results obtained were not significant, the use of HCl as an activator was still better than H_2SO_4.

4. Conclusion

ONC characterization showed that the samples contain montmorillonite and quartz; there was an increase in the essential distance of pure ONC samples from 3.32232 Å to 3.33769 Å for 3 M ONC-HCl, which was caused by the process of dealumination and deionization. The dealumination process was supported by IR data where there is a shift in wave number in the Al-O stretching vibration region (796-794 cm⁻¹) and a sharper vibration in the Si-O region (488-468 cm⁻¹). Si/Al ratio also supported the process of dealumination, in which the pure ONC sample ratio increased from 1.7497 to 2.2970 for 3 M ONC-HCl. The concentration of the hydrochloric acid did not affect the capacity of ONC as an adsorbent for methylene blue. The adsorption capacity of pure ONC obtained was 4.97215 mg/g, while for 3 M ONC-HCl, it was 4.97746 mg/g.

References

[1] Krishna G. Bhattacharyya, Susmita Sen Gupta, Kaolinite, montmorillonite, and their modified derivatives as adsorbents for removal of Cu(II) from aqueous solution, *Separation and Purification Technology*, 50, 3, (2006), 388-397 https://doi.org/10.1016/j.seppur.2005.12.014

[2] P. Suarya, Adsorpsi Pengotor Minyak Daun Cengkeh oleh Lempung Teraktivasi Asam, *Jurnal Kimia (Journal of Chemistry)*, 2, 1, (2012), 19-24

[3] Bijang Catherina, Wahab Abd. Wahid, Maming, Ahmad Ahyar, Taba Paulina, Design of Bentonite Acid Modified Electrodes in Cyanide Biosensors, *International Journal of Materials Science and Applications*, 4, 2, (2015), 115-119 https://doi.org/10.11648/j.ijmsa.20150402.17

[4] Abdelfattah Amari, Hatem Gannouni, Mohammad I. Khan, Mohammed K. Almesfer, Abubakr M. Elkhaleefa, Abdelaziz Gannouni, Effect of Structure and Chemical Activation on the Adsorption Properties of Green Clay Minerals for the Removal of Cationic Dye, *Applied Sciences*, 8, 11, (2018), 2302 https://doi.org/10.3390/app8112302

[5] Frida Ayu Malini, Endah Mutiara Marhaeni Putri, Kinetika Oksidasi Fotokatalitik Metilen Biru dengan Katalis Semikonduktor TiO₂, *Jurnal Sains dan Seni Pomits*, 2, 1, (2014), 1-7

[6] Jemal Mohammed Yassin, Yoseph Shiferaw, Abebe Tedla, Application of acid activated natural clays for improving quality of Niger (*Guizotia abyssinica* Cass) oil, *Heliyon*, 8, 4, (2022), e09241 https://doi.org/10.1016/j.heliyon.2022.e09241

[7] M. Loutfi, R. Mariouch, I. Mariouch, M. Belfaquir, M. S. ElYoubi, Adsorption of methylene blue dye from aqueous solutions onto natural clay: Equilibrium and kinetic studies, *Materials Today: Proceedings*, 72, (2023), 3638-3643 https://doi.org/10.1016/j.matpr.2022.08.412

[8] Mahammedi Fatiha, Benguella Belkacem, Adsorption of methylene blue from aqueous solutions using natural clay, *Journal of Materials and Environmental Sciences*, 7, 1, (2016), 285-292

[9]   B. Damiyine, A. Guenbour, R. Boussen, Rhodamine B adsorption on natural and modified Moroccan clay with cetyltrimethylammonium bromide: Kinetics, equilibrium and thermodynamics, *Journal of Materials and Environmental Sciences*, 8, 3, (2017), 860-871

[10] Will Gates, J. Theo Kloprogge, Jana Madejova, Faïza Bergaya, *Infrared and Raman spectroscopies of clay minerals*, 1st ed., Elsevier, 2017,

[11] J. Madejová, FTIR techniques in clay mineral studies, *Vibrational Spectroscopy*, 31, 1, (2003), 1-10 https://doi.org/10.1016/S0924-2031(02)00065-6

[12] R. E. Grim, *Clay Mineralogy*, McGraw-Hill, University of Minnesota, 1968,

[13] Kovo G. Akpomie, Folasegun A. Dawodu, Acid-modified montmorillonite for sorption of heavy metals from automobile effluent, *Beni-Suef University Journal of Basic and Applied Sciences*, 5, 1, (2016), 1-12 https://doi.org/10.1016/j.bjbas.2016.01.003

[14] Ingrid Wilke, Vidya Ramanathan, Julienne LaChance, Anthony Tamalonis, Michael Aldersley, Prakash C. Joshi, James Ferris, Characterization of the terahertz frequency optical constants of montmorillonite, *Applied Clay Science*, 87, (2014), 61-65 https://doi.org/10.1016/j.clay.2013.11.006

[15] Anne Julbe, Chapter 6 - Zeolite Membranes – Synthesis, Characterization and Application, in: J. Čejka, H. van Bekkum, A. Corma, F. Schüth (Eds.) *Studies in Surface Science and Catalysis*, Elsevier, 2007, https://doi.org/10.1016/S0167-2991(07)80794-4

[16] Lynne B. McCusker, Christian Baerlocher, Chapter 2 - Zeolite Structures, in: J. Čejka, H. van Bekkum, A. Corma, F. Schüth (Eds.) *Studies in Surface Science and Catalysis*, Elsevier, 2007, https://doi.org/10.1016/S0167-2991(07)80790-7

[17] Jihong Yu, Chapter 3 - Synthesis of Zeolites, in: J. Čejka, H. van Bekkum, A. Corma, F. Schüth (Eds.) *Studies in Surface Science and Catalysis*, Elsevier, 2007, https://doi.org/10.1016/S0167-2991(07)80791-9

[18] Johannes A. Lercher, Andreas Jentys, Chapter 13 - Infrared and Raman Spectroscopy for Characterizing Zeolites, in: J. Čejka, H. van Bekkum, A. Corma, F. Schüth (Eds.) *Studies in Surface Science and Catalysis*, Elsevier, 2007, https://doi.org/10.1016/S0167-2991(07)80801-9

[19] Müşerref Önal, Yüksel Sarıkaya, Preparation and characterization of acid-activated bentonite powders, *Powder Technology*, 172, 1, (2007), 14-18 https://doi.org/10.1016/j.powtec.2006.10.034

[20] Krishna G. Bhattacharyya, Susmita Sen Gupta, Uptake of Ni(II) Ions from Aqueous Solution by Kaolinite and Montmorillonite: Influence of Acid Activation of the Clays, *Separation Science and Technology*, 43, 11-12, (2008), 3221-3250 https://doi.org/10.1080/01496390802219638

[21] Peter Komadel, Acid activated clays: Materials in continuous demand, *Applied Clay Science*, 131, (2016), 84-99 https://doi.org/10.1016/j.clay.2016.05.001